DEUTSCHES ELEKTRONEN – SYNCHROTRON DESY

DESY SR 87-05
July 1987

THE ADSORPTION SITE OF OXYGEN ON SI(100) DETERMINED BY SEXAFS

by

L. Incoccia, A. Balerna

Hamburger Synchrotronstrahlungslabor HASYLAB at DESY

S. Cramm, C. Kunz, F. Senf, I. Storjohann

II. Inst. f. Experimentalphysik, Universität Hamburg

ISSN 0723-7979

NOTKESTRASSE 85 · 2 HAMBURG 52

DESY SR 87-05
July 1987

ISSN 0723-7979

The adsorption site of oxygen on Si(100) determined by SEXAFS

L. Incoccia and A. Balerna
HASYLAB at DESY, Notkestr. 85, D-2000 Hamburg 52

S. Cramm, C. Kunz, F. Senf and I. Storjohann
II. Inst. für Experimentalphysik, Universität Hamburg,
Luruper Chaussee 149, D-2000 Hamburg 50

We present a SEXAFS (Surface Extended X-Ray Absorption Fine Structure) investigation of oxygen adsorbed on Si(100) at the oxygen K absorption edge (E_K = 535 eV) in the photon energy range 500-800 eV. The oxygen uptake on Si(100) at room temperature reaches a saturation at about one monolayer coverage, where the (2x1) reconstruction of the clean surface is lost. Our results demonstrate the following: the oxygen atoms occupy two types of bridge positions, namely between Si atoms belonging to the first layer and between Si atoms belonging to different topmost layers. The bridge site is characterized by a bond distance of 1.65 Å and a Si-O-Si bond angle of ≈ 120°. No evidence of other types of adsorption geometries is found nor the presence of adsorbed molecular oxygen is observed.

Proc. ECOSS-9 Conf., Luzern, 1987, to be published in Surf. Sci.

ISSN 0723-7979

The work done in the last years, both theoretical and experimental, yielded a considerable insight into the mechanism of oxidation of Si surfaces.

Coverage studies (1) identified a fast RT adsorption phase, which takes place between 1 and ≈ 100 Langmuir (1 Langmuir = 1 L = 10^{-6} Torr s) oxygen exposure and results in a first saturation coverage of slightly more than one monolayer, followed by a much slower oxygen uptake, which is assumed to correspond to the oxygen penetrating into the bulk.

However, the mechanism of the early stage of silicon oxidation, the question whether the oxygen sticks on to the surface as a molecule or as an atom (or both), the possible configuration of the adsorption site: all those points have been the subject of longstanding debates. From LEED studies of oxygen on Si(100) we know that upon oxygen exposure, the (2x1) reconstruction of the clean surface slowly disappears at coverages which are somewhat contradictory in the literature, ranging from 20 L O_2 to 100 L O_2 or more, whereas a (1x1) LEED pattern is still present. Photoemission data (2) proved that the first RT adsorbed phase does not correspond to the formation of a stoichiometric oxide. Hollinger and Himpsel (2) observed shifted surface Si 2p peaks, and interpreted them as due to silicon in coordination with mainly one or two oxygen atoms. From EELS experiments Ibach et al. (3) indicated the bridge position as the most probable one for the oxygen atom, but they explicitly rule out the first layer bridge position on the basis of symmetry considerations. Moreover, they cannot exclude the presence of adsorbed molecular species. More recently Schaefer et al. (4) could interpret their XPS and EELS spectra in terms of Si-O-Si complexes only, and gave an estimate of the bonding angle using a central-force model. On the theoretical side, Batra et al. (5) showed that the dissociative adsorption of O_2 on Si(100) is energetically favoured, and that the first-layer bridge position is more stable than the on-top position, but conclude that both configurations are possible.

In this work, we present a structural study of the room temperature adsorption of oxygen on Si(100) using SEXAFS, at the end of the fast adsorption phase, where the first saturation is reached. At this coverage the (2x1) reconstruction is lost already, indicating the presence of a thin perturbed phase (at most 2-3 monolayers thick) on the still ordered Si bulk underneath. SEXAFS, being a local structural probe, is the appropriate technique to give a more detailed description of the absorption site.

Experimental

The samples, thin Si wafers, were mounted in a UHV chamber 2×10^{-10} torr) onto a heatable sample holder. The manipulator axis coincides with the direction of the incoming beam, allowing an easy variation of the angle between the $\vec{E}$ vector and the normal to the surface.

The Si surfaces were prepared with repeated cycles of mild sputtering and annealing ($T \approx 950^{\circ}C$). The samples were then checked for cleanliness and quality of the surface by Auger and photoemission spectroscopy and LEED. O_2 gas was introduced into the vacuum chamber through a leak valve up to a pressure of 1×10^{-8} - 5×10^{-8} torr. The intensity of the photon excited oxygen Auger KLL peak was used to monitor the oxygen uptake. Saturation coverage was reached at about 40 L.

The experiments were carried out with the FLIPPER monochromator at the wiggler/undulator beamline at HASYLAB (6) using synchrotron radiation of the storage ring DORIS. An average resolution of $\Delta E = 1.5$ eV was used. The absorption spectra in the range of the oxygen K edge were measured in the 500-800 eV photon energy range using a total electron yield detection scheme before and after the oxygen exposure (I_{clean} and I_{ox} respectively). I_{clean} represents the background signal due to the silicon bulk. The final surface EXAFS spectrum was obtained as I_{ox}/I_{clean}. These spectra were taken at two different angles with respect to the $\vec{E}$ vector: s - polarization ($\vec{E}$ lying in the surface) and p - polarization ($\vec{E}$ orthogonal to the surface), both at grazing incidence angle. As a reference spectrum for the EXAFS phase shifts we measured a thin film (60 Å) of vitreous SiO_2.

Results and Discussion

The SEXAFS $\chi(k)$ functions in s- and p-polarization, extracted from the experimental data using a standard procedure (7), are reported in fig. 1, together with their Fourier transforms. A first inspection of the spectra shows no polarization dependence of frequency and amplitude of the EXAFS oszillations within the experimental accuracy, allowing the exclusion of on top positions and molecularly adsorbed species. An adsorbed molecule should give rise to specific resonances close to the edge besides showing up at shorter distances in the Fourier-Transform of the EXAFS spectrum. The inverse Fourier transform of the first peak was used to yield the total scattering phase $\Phi(k)$ and the total backscattering amplitude $A(k)$.

A comparison of $\Phi(k)$ with the total phase pertaining to a-SiO_2($\Phi_M(k)$) over the whole experimental k-range results in a O-Si nearest neighbour (n.n.) distance of:

$$R = 1.65 \pm 0.02 \text{ Å} \quad .$$

The uncertainty of this result is mainly due, more than to the signal-to-noise ratio, which is in our case extremely satisfactory, to the procedure necessary to extract the oscillatory function. We want to underline here that the good linear behaviour of the function $\Delta R(k) = \Phi_M(k) - \Phi(k)$ is already an indication that we are dealing with a single n.n. shell (7). This leads to the conclusion that only <u>one type</u> of adsorption site is present on the surface. This statement is proved by means of a χ (k)-fit, assuming one shell and the n.n. distance given above, being in excellent agreement with the data.

To proceed further, we have now to analyze the amplitudes of the spectra. The behaviour of the intensity of the spectra (or, in other words, of the coordination numbers) as a function of the polarization gives us information on other geometrical parameters, e.g. bond angles. The effective coordination number N* in a SEXAFS experiment is defined by (see (7)):

$$N^* = 3 \sum_j \cos^2 \alpha_j \qquad j = \text{neighbour} \qquad (1)$$

where α_j is the angle between the $\vec{E}$ vector and the bond direction $\vec{R}_j$. The value of α_j must be evaluated for each specific structural model one wants to test.

As already mentioned, the most probable geometry of the adsorbed oxygen is a bridge position, with the oxygen sitting on the vertex of an isosceles triangle, as shown in fig. 2. The angle δ of fig. 2 describes the inclination of the triangle with respect to the ideal Si(100) surface, and assumes different values if the oxygen is connecting two first-layer Si atoms (i.e. the asymmetric dimer proposed by Chadi (8)) or, for example, first-second layer Si atoms. The angle η of fig. 2 is simply related to the bond angle ϑ of the Si-O-Si complex by:

$$\vartheta = 180^{\circ} - 2\,\eta \quad .$$

From eq. 1 we obtain for the effective coordination numbers in s- and p-polarization:

$$\begin{aligned} N^*_s &= (3/2)\,[\cos^2(\eta-\delta) + \cos^2(\eta+\delta)] \\ N^*_p &= 3\,[\sin^2(\eta-\delta) + \sin^2(\eta+\delta)] \quad , \end{aligned} \qquad (2)$$

where we already averaged over $\cos^2\varphi$, φ being the azimuthal angle on the surface.

In our case, in fact, φ is not uniquely defined, as can already be deduced from the LEED picture of the clean (100) surface which shows the presence of two (2x1) domains rotated by 90°. Moreover the (2x1) long range order is washed out and finally disappears during oxygen uptake.

In principle, we could separately measure N^*_s and N^*_p, thus obtaining a unique determination of η and δ. This is unfortunately rendered very problematic by the lack of the proper EXAFS model for the amplitudes. We prefer to rely on the ratio of the effective coordination numbers N^*_s/N^*_p, which is model-independent.

Our experimental data yield: $N^*_s/N^*_p \approx 1$. Considering this, we can transform eq. 2 to:

$$\cos(2\delta) = 1/3\cos(2\eta) \qquad (3)$$

The resulting $\eta(\delta)$-plot is shown in fig. 3, together with the corresponding R(Si-Si).

In order to interpret this result, let us first remind that at the saturation coverage of roughly 1 ML, not only the first-layer bridge

position ($\delta = 10^{\circ}$) will be occupied, but at least an equal number of similar positions between the topmost layers ($\delta = 35^{\circ}$) is needed in order to explain the oxygen uptake. If we assume that the presence of oxygen does not dramatically distort the angle δ, then we obtain for δ an average value of $\approx 23^{\circ}$ (marked 'a' in fig. 3). This yields in turn $\eta = 30^{\circ}$ and consequently a bond angle ϑ of 120°. On the other hand, if we take from ref. 4 the ϑ-value for the room temperature saturation coverage, $\vartheta = 124^{\circ}$ (and consequently $\eta = 28^{\circ}$, marked 'b' in fig. 3), we deduce from our data a $\delta = 27^{\circ}$. Our results are then not only fully in accordance with photoemission and vibrational spectroscopies, as well as with theoretical calculations, but they prove also that the oxygen occupies both types of bridge positions ($\delta = 10^{\circ}$ and $\delta = 35^{\circ}$).

Furthermore, we want to underline that we do not need to invoke the presence of another adsorption geometry in order to explain our data. In particular, we do not observe any evidence of the presence of molecular oxygen on the surface. Using the above values for ϑ and our experimentally determined O-Si distance of 1.65 Å, we get a Si-Si distance in the range 2.86 - 2.91 Å, which implies a relatively small amount of strain introduced by the oxygen. This is in turn the most reasonable explanation of the presence of the (1x1) LEED pattern at oxygen saturation.

This work has been funded by the German Federal Minister for Research and Technology (BMFT) under contract number 05 305 AX B, Teilv. 3.

Figure Captions

Figure 1

a) EXAFS functions $\chi(k)$ at the oxygen K edge for s- and p-polarization, obtained after subtraction of a polynomial fit representing the atomic-like absorption. The origin of the k scale has been taken at the inflection point of the absorption edge.

b) Fourier transform of the above spectra in the k range 2-8 $Å^{-1}$. A k^2 weighting factor was used. In order to get the real O - Si distance a phase shift has to be taken into account.

Figure 2

The Si-O-Si complex can be represented as a triangle whose basis (the Si-Si line) form an angle δ with the surface.

Figure 3

$\eta(\delta)$-plot according to eq. 3, which considers the experimental result $N^*_s = N^*_p$ and simple trigonometric considerations. Values marked as 'a' and 'b' are explained in the text.

References

(1) W. Ranke and Y.R. Xing
Surface Sci. 157 (1985) 353

(2) G. Hollinger and F.J. Himpsel
Phys. Rev. B28 (1983) 3651

(3) H. Ibach, H.D. Bruchmann and H. Wagner
Appl. Phys. A29 (1982) 113

(4) J.A. Schaefer and W. Göpel
Surface Sci. 155 (1985) 535

(5) I.P. Batra, P.S. Bagus and K. Hermann
Phys. Rev. Lett. 52 (1984) 384

(6) F. Senf, K.B. v. Rautenfeld, S. Cramm, J. Lamp, J. Schmidt-May, J. Voss, C. Kunz and V. Saile
Nucl. Instr. Meth. A246 (1986) 314

(7) For a complete discussion of the EXAFS data analysis and formalism see e.g.: J. Stöhr, in: Principles, Techniques and Applications of EXAFS, SEXAFS and XANES, eds. D. Koningsberger and R. Prins (Wiley, New York, 1984)

(8) D.J. Chadi, Phys. Rev. Lett. 43 (1979) 43

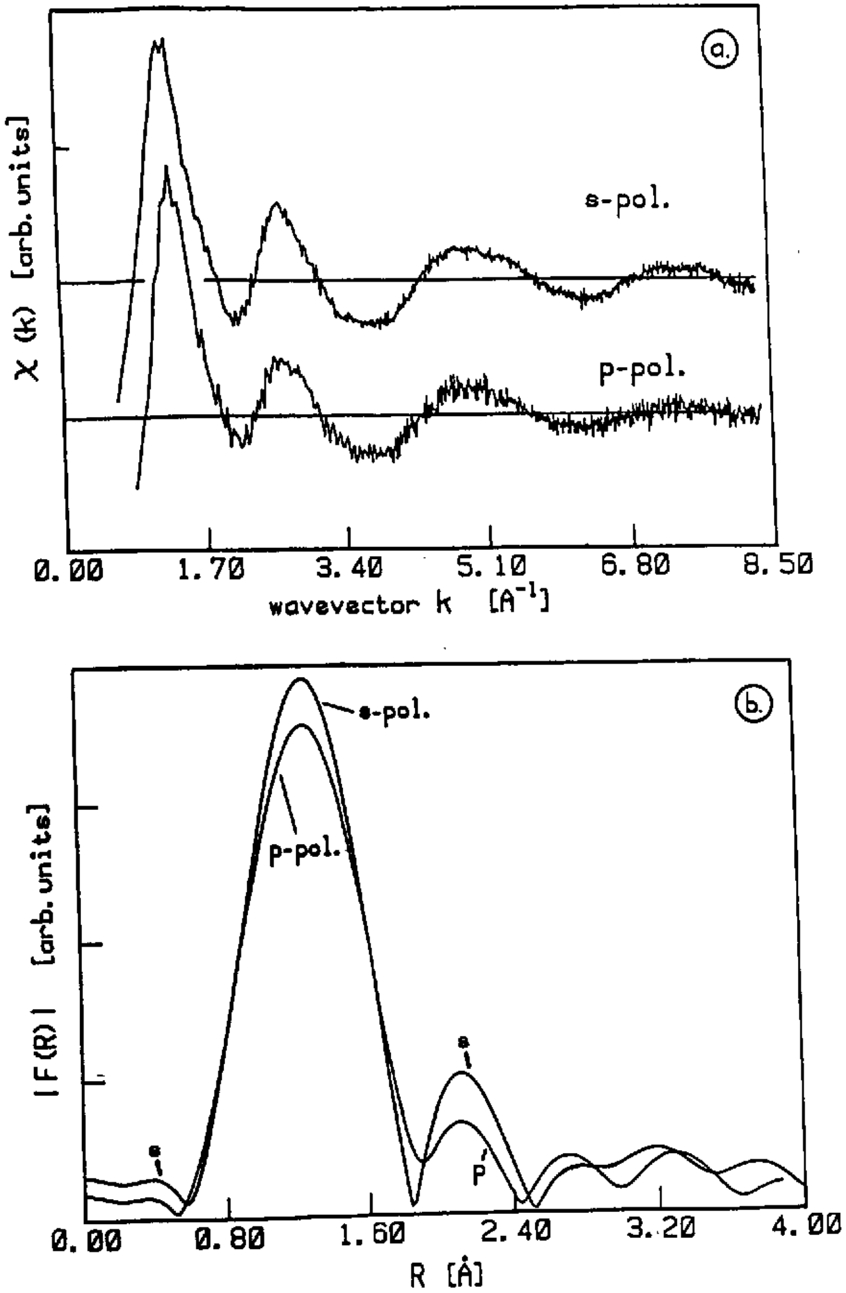
a.
s-pol.
p-pol.
χ (k) [arb. units]
0.00
1.70
3.40
5.10
6.80
8.50
wavevector k [Å^{-1}]
b.
s-pol.
p-pol.
s
s
p
|F(R)| [arb. units]
0.00
0.80
1.60
2.40
3.20
4.00
R [Å]

FIG. 1

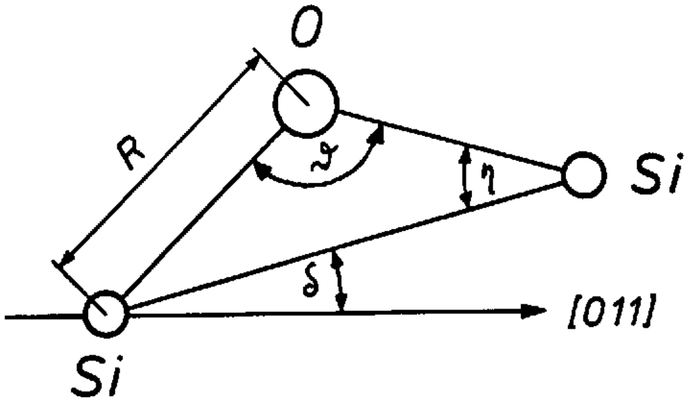
O
R
ϑ
η
Si
δ
[011]
Si

FIG. 2

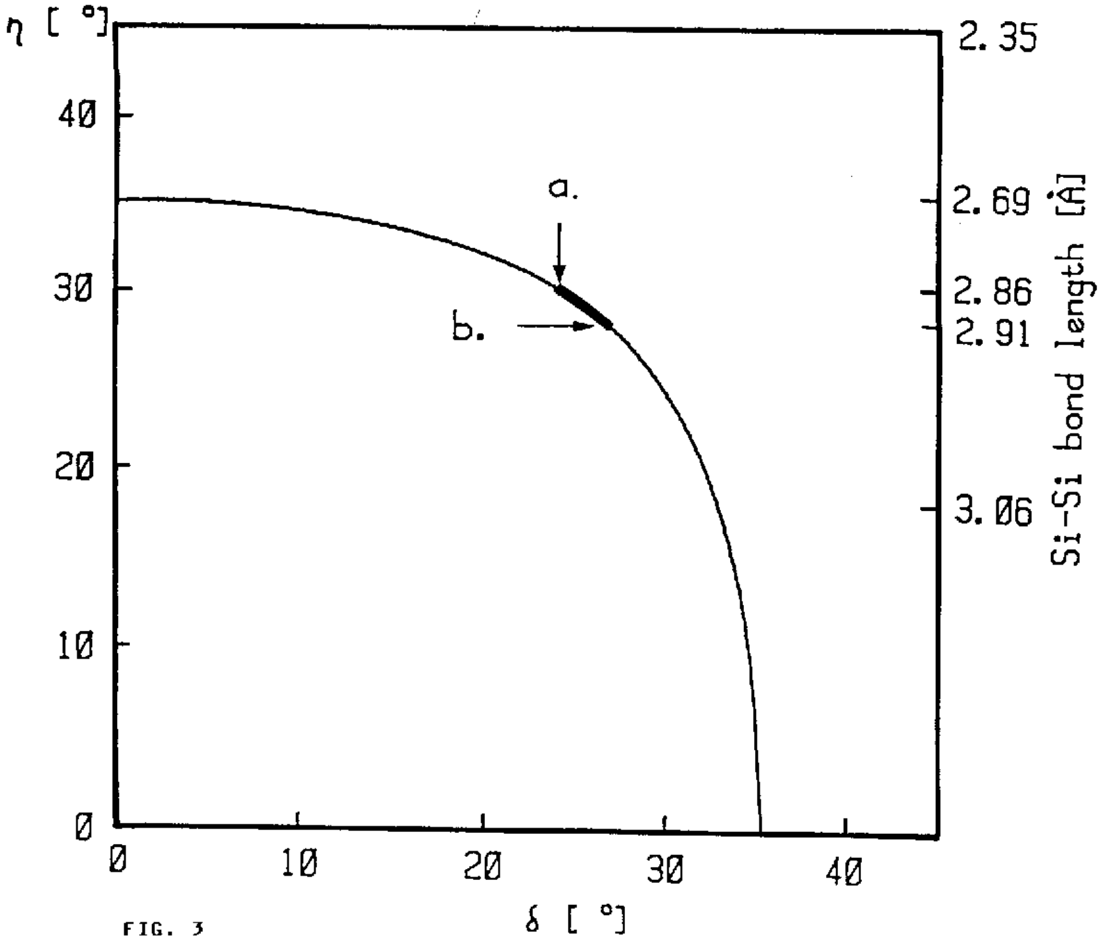
η [°]
40
30
20
10
0
0
10
20
30
40
δ [°]
a.
b.
2.35
2.69
2.86
2.91
3.06
Si-Si bond length [Å]

FIG. 3